Title: How does the cell wall 'stick' in the mucilage? A detailed microstructural analysis of the seed coat mucilaginous cell wall

Authors: Agnieszka Kreitschitz, Stanislav N. Gorb

PII: S0367-2530(17)33131-6
DOI: http://dx.doi.org/doi:10.1016/j.flora.2017.02.010
Reference: FLORA 51080

To appear in:

Received date: 2-6-2016
Revised date: 25-1-2017
Accepted date: 8-2-2017

Please cite this article as: Kreitschitz, Agnieszka, Gorb, Stanislav N., How does the cell wall 'stick' in the mucilage? A detailed microstructural analysis of the seed coat mucilaginous cell wall.Flora http://dx.doi.org/10.1016/j.flora.2017.02.010

How does the cell wall 'stick' in the mucilage? A detailed microstructural analysis of the seed coat mucilaginous cell wall

Agnieszka Kreitschitz [1,2*] and Stanislav N. Gorb[2]

[1] Department of Plant Developmental Biology, Institute of Experimental Biology, University of Wrocław, ul. Kanonia 6/8, 50-328, Wrocław, Poland.

[2] Department of Functional Morphology and Biomechanics, Kiel University, Am Botanischen Garten 1-9, D-24098 Kiel, Germany, sgorb@zoologie.uni-kiel.de

* For correspondence: e-mail: agnieszka.kreitschitz@uwr.edu.pl (tel. +48 71 375 40 91, fax: +48 71 375 41 18)

Highlights

- Microstructural organization of mucilaginous cell wall is direct visualized
- Characteristic net-like architecture of the seed mucilage envelope is demonstrated
- Immunolocalizations show the presence of selected hemicelluloses in the mucilage

Abstract

The seed mucilage envelope of myxospermatic diaspores is considered as a modified cell wall. Its chemical constitutes are mainy polysaccharide groups typical of the cell wall, however, pectins are very often the main component. A detailed analysis of the mucilaginous cell wall spatial architecture was demonstrated for the first time using a less-invasive CPD+SEM technique, which allowed the preservation of the mucilaginous cell wall structure. The examined pectic (*Linum usitatissimum*) and cellulose (*Neopallasia pectinata*) seed mucilage showed the fibrillary character of the components. The second type of mucilage indicated a much more arranged structure than that of the pectic one due to the presence of cellulose microfibrils. We showed cellulose organization in a net-like scaffold on which other mucilage components were spread and shoved how the mucilage was anchored to the seed surface through the cellulose skeleton, preventing it from being lost. Our detailed analysis gave an insight into how the mucilage is spatially arranged and also provided direct microstructural evidence of cell wall polysaccharides structure, distribution and interactions especially for widely-postulated xylan-cellulose linking. We demonstrated that xylan might be represented by long chains covering the surface of cellulose fibrils. The main advantage of the applied technique is its less-invasive character which retains the 3D structure of the components within the intact mucilaginous cell wall. As utilized in our studies, preparation and visualization methods with seed mucilage as a model system can give us new possibilities in structural studies of the (mucilaginous) cell wall.

Keywords: cell wall, hemicelluloses, seed mucilage, *Neopallasia pectinata*, *Linum usitatissimum*.

1. Introduction

The plant cell wall (CW) is involved in different processes which maintain the proper functioning of cell and plant survival. Such processes range from the control of cell expansion, transport regulation, enhancing mechanical strength, maintaining cell shape and defending the cell against pathogens to signal transduction and cell adhesion. Cell wall structure and composition differ between the primary (PCW) and secondary cell wall (SCW) and can continually be modified as a a result of diverse environmental conditions (Bidlack et al., 1992; Caffal and Mohnen, 2009; Banasiak, 2014).

The typical plant cell wall of dicotyledonous plants is a complex structure composed of three main groups of polysaccharides: cellulose, pectins and hemicellulose linked together by different bonds in the form of a spatial network (Somerville et al., 2004; Zykwinska et al., 2005, 2007; Donaldson, 2007; Jarvis, 2011). However, such a composition is more typical of the PCW, whereas the SCW mainly consists of cellulose and hemicelluloses and appears to be more structurally organized than the PCW in this instance (Bidlack et al., 1992). The size of cellulose microfibrils can differ between diverse plants and cell wall types (PCW, SCW). The width of a microfibril was assessed at 8-15 nm (McCain et al., 1990; Fujino et al., 2000). Microfibrils can aggregate forming bundles (macrofibrils) of different size e.g. 12-24 nm or even from 50 to 250 nm (Ding and Himmel, 2006; Donaldson, 2007; Terashima et al., 2009; Ding et al., 2013).

The difference between the PCW and SCW also involves hemicellulose constitution. One of the most important hemicelluloses in the primary cell wall is xyloglucan (XG), whereas xylan (XY) and arabinoxylan are less substituted polymers, characteristic of the secondary cell walls in dicots (Zykwinska, 2007; Sheller and Ulskov, 2010; Banasiak, 2014; Busse-Wicher et al., 2014; Cosgrove, 2014). Pectins are linear or branched (with attached side chains) polymers of galacturonic acid residues, they are characteristic of the primary cell wall in all land plants and play diverse roles in wall structure and function (Willats et al., 2001; Pelloux et al., 2007; Mohnen, 2008; Caffal and Mohnen, 2009; Banasiak, 2014). The most abundant pectic polysaccharide is homogalacturonan (HG) which represents a linear, unbranched homopolymer of galacturonic acid. Other important pectins of the cell wall are rhamnogalacturonan II and/or rhamnogalacturonan I (RG I) the backbone of which is composed of repeat disaccharides i.e. rhamnose and galacturonic acid (Mohnen, 2008).

Mucilage secreting cells (MSCs) are characteristic of many types of fruit and seeds able to produce a mucilage envelope after hydration. This phenomenon, known as myxodiaspory, is a common adaptation to drought habitats in many families of angiosperms

(Grubert, 1974; Kreitschitz, 2009; Kreitschitz, 2012). Soon after hydration, the mucilage secreting cell walls burst, loosening their material in the form of an easily accessible, gel-like envelope (Arsovski et al., 2010; Haughn and Western, 2012; Kreitschitz, 2012). The mucilage envelope is characterized by a complex composition and structure and could be considered as a specialized pectin-rich secondary cell wall (Haughn and Western, 2012). Mucilage composed mainly of pectins and hemicelluloses is known as pectic ('true') mucilage typical of *Linum* sp. The second type has additional cellulose fibrils and was described as cellulose mucilage characteristic of many diverse families such as Asteraceae, Brassicaceae, Lamiaceae or Plantaginaceae (Western, 2012; Kreitschitz et al., 2009; Kreitschitz, 2012). As the seed coat of *Arabidopsis thaliana*, a model plant, is amenable to genetic manipulation and due to the special character of its mucilage, it has been adapted to diverse studies of the functional aspects of the cell wall (Haughn and Western, 2012; North et al., 2014; Voiniciuc et al., 2015a). Although our knowledge of seed coat mucilage composition, function and development is quite extensive, the detailed structural, spatial organization of the mucilage components still remains unclear (Macquet et al., 2007; Mendu et al., 2011; Sullivan et al., 2011; Haughn and Western, 2012).

Mucilage lacking cellulose fibrils is also regarded as primary-cell-wall-like, whereas the cellulose type is regarded as a specific, modified secondary cell wall (Mühlethaler, 1950; Haughn and Western, 2012; Western, 2012). This separation is derived from a number of immuno- and biochemical analyses of mucilage components which showed the presence of hemicelluloses such as arabinoxylan and xyloglucan typical of the PCW (Naran et al., 2008; Young et al., 2008; Arsovski et al., 2009). In the case of cellulose mucilage regarded as a modified SCW, the presence of xylan, typical of this type of cell wall was also shown (Ralet et al., 2016; Voiniciuc et al., 2015b; Xu et al., 2016 a, b).

Our knowledge of the distribution of mucilage components' within the mucilage envelope is derived mainly from biochemical analysis (Naran et al., 2008; Young et al., 2008; Arsovski et al., 2009; Western, 2012; Voiniciuc et al., 2015 a, b). Another question is the spatial organization of mucilage polysaccharides – does it reflect cell wall arrangement?

Cell wall structure has been examined with diverse microscopy techniques including Atomic Force Microscopy (AFM), Transmission and Scanning Electron Microscopy (TEM, SEM), and Cryo-SEM. They have revealed the fibrillary nature of cell wall components and such analyses have largely been based on the use of invasive sample preparations such as enzymatic or chemical treatments, which can destroy and/or influence cell wall organization and its individual components (McCann et al., 1990; Satiat-Jeunemaitre et al., 1992; McCann

and Roberts, 1991; Nakashima et al., 1997; Zykwinska et al., 2007; Sarkar et al., 2009; Terashima et al., 2009; Sarkar et al., 2014). Some general micromorphological studies of seed coat mucilage envelope(s) using SEM analysis were also presented e.g. for nutlets of *Salvia hispanica* L. or *Arabidopsis thaliana* seeds (Windsor et al., 2000; Capitani et al., 2013; Salgado-Cruz et al., 2013; Voiniciuc et al., 2013). However, these studies did not give a detailed insight into the spatial architecture of the mucilage.

Our previous studies on the mucilaginous seeds of selected Asteraceae taxa and *Neopallasia pectinata* allowed us to classify the mucilage according to the cellulose type. Pectins and cellulose were very distinctive components, organized in a smaller or abundant mucilage envelope (Kreitschitz and Vallès, 2007; Kreitschitz, 2012). Taking our results into account, we decided to examine seeds of *Neopallasia pectinata*, which produce abundant cellulose mucilage with very long, complexed cellulose fibrils (Kreitschitz and Vallès, 2007). The second selected plant species is flax *Linum usitatissimum* whose seeds produce pectic mucilage which is a mixture of branched rhamnogalacturonan I and arabinoxylan and lacks cellulose (Naran et al., 2008).

The main aim of this study was to analyze and visualize the spatial structural organization of the seed coat mucilage (seed coat mucilaginous cell wall) of two taxa differing in mucilage composition and morphology i.e. *Linum usitatissimum* with pectic mucilage and *Neopallasa pectinata* with cellulose mucilage. To explore the mucilage spatial organization, we applied less-invasive techniques i.e. critical point drying (CPD) followed by high resolution scanning electron microscopy (SEM). We also analyzed the presence of selected hemicelluloses i.e. xylan/arabinoxylan and xyloglucan whose occurrence was described for the mucilaginous cell wall.

2. Material and methods

Mature seeds of *Neopallasia pectinata* were obtained from Prof. Dr. Joan Vallès (Barcelona University, Catalonia, Spain). The seeds of *Linum usitatissimum* (flax) were obtained from a commercial supplier (SANTE, A. Kowalski Sp. j., Warsaw, Poland). The material for CPD and SEM analysis were not fixed in any special fixative solution and not chemically or enzymatically pretreated.

2.1. Morphology of the mucilage envelope - pectins and cellulose detection.

In order to detect the main mucilage components staining with ruthenium red (0.1%, w/v) for pectins, with safranin (0.1%, w/v) for cellulose and pectins and with Direct Red 23 (0,1% w/v) for cellulose (excitation LP 555, emission 560 nm) were done. Images were taken

using a DP71 camera connected to an Olympus BX-50 microscope and Cell B imaging software (Olympus BX50, Olympus Optical Co, Poland) and with Zeiss CLSM microscope (LSM 700 AXIO ZEISS; staining with Direct Red 23). Additionally, in order to observe the presence of crystalline cellulose a polarized light microscope was used. The highly ordered cellulose microfibrils present in the mucilage envelope can produce birefringence of polarized light (Sullivan et al., 2011; Yu et al., 2014). A Leica polarized light microscope connected to a Leica DFC 450 C camera and Las X software (Leica DM 6000B, Leica Microsystems GmbH, Germany) was used.

2.2. Examination of seed coat mucilage arrangement in dry seeds

Handmade cross-sections of *N. pectinata* dry seeds were attached to the SEM stubs using carbon-containing double-sided adhesive conductive tape and coated with gold palladium (film thickness 15 nm) using a Leica EM SCD 500 High Vacuum Sputter Coater (Leica Microsystems GmbH, Wetzlar, Germany). The preparations were visualized in a SEM (Hitachi S-4800, Hitachi High-Tech. Corp., Tokyo, Japan).

2.3. Examination of the morphology of dried seed coat mucilage

Round cover slips of the same size were attached to the SEM stubs using double carbon-containing double-sided adhesive conductive tape. Next, seeds of both plant species (after 30 min of hydration) were put individually on these cover slips and air-dried for 24 h. Samples were coated with gold palladium (film thickness 10 nm) using a Leica EM SCD 500 High Vacuum Sputter Coater (Leica Microsystems GmbH, Wetzlar, Germany) and visualized in a SEM (Hitachi S-4800, Hitachi High-Tech. Corp., Tokyo, Japan).

2.4. Examination of the spatial organization of seed coat mucilage in hydrated and CPD-dried seeds

Seeds of both plant species were hydrated for 30 min to obtain a mucilage envelope, and were then dehydrated in an ascending ethanol series from 10% to 100%. After that, the seeds were dried using a critical point dryer (Typ E 3000, United Kingdom, Quorum Technologies Ltd, Unit 15a Euro Business Park New Road, New Haven, East Sussex, England), mounted on the SEM-stubs, coated with gold palladium (film thickness 10 nm) and immediately visualized in the SEM.

2.5. Localization of xylan/arabinoxylan and xyloglucan epitopes by immunolabeling

Taking some previous biochemical and morphological studies (and experiments) on mucilage composition and structure into consideration (Naran et al., 2008; Kreitschitz, 2012) we selected two specific monoclonal antibodies.

Two primary monoclonal antibodies were used for the studies: LM11 (Plant Probes, Leeds, UK), which recognizes unsubstituted and relatively low-substituted xylan and arabinoxylan (McCartney et al., 2005) and LM15 (Plant Probes, Leeds, UK), which recognizes the XXXG motif of xyloglucan (Marcus et al., 2008). Intact mature seeds were hydrated in water for 30 min to obtain the mucilage envelope. The mucilaginous seeds were fixed for 1 h in 4% (w/v) paraformaldehyde. Samples were washed with PBS (3 x 5 min) and incubated in blocking buffer (Skim Milk Powder, Fluka, BioChemika, Switzerland) for 1 h. Afterward, the monoclonal antibodies were applied (diluted 1:10 in PBS) and incubated over night at 4°C in a humid chamber. The samples were washed with PBS (5 x 3 min) and the secondary antibody (Anti-Rat IgG FITC, Sigma, St. Louis, USA) (diluted 1:100 in PBS) was applied. The samples were incubated overnight at 4°C in darkness. Samples were washed with PBS (5 x 3 min) and mounted in a mixture of PBS with glycerin. To detect and visualize cellulose fibrils in the same samples, they were first labeled with the LM11 antibody (as described above). The observations were done using an Olympus BX-50 epi-fluorescent microscope with a blue light excitation filter (470-490 nm). The following control probes were used: 1. Autofluorescence of the sample. 2. Control – only with a secondary antibody. 3. Control - only with a primary monoclonal antibody. Images were taken using a DP71 camera connected to an Olympus BX-50 microscope with epifluorescence and Cell B imaging software (Olympus BX50, Olympus Optical Co, Poland).

3. Results

3.1. Mucilage characteristics

Mucilage of *Linum usitatissimum* formed an irregular envelope around the seed (Fig. 1 A-C), consiststing mainly of pectins (Fig. 1 B-C). The mucilage width ranged from 50 to about 300 μm. The mucilage of *Neopallasia pectinata* was very abundant, in comparison to *L. usitatissimum*, and formed very wide envelope (about 1 mm width) (Fig. 1 D-J). The main component were pectins (Fig. 1 D) in which long cellulose fibrils were spread. The cellulose fibrils were well visible after staining with safranin (Fig. 1 F-H). They could stay coiled at the end (Fig. 1 G-H) forming a thicker layer in which the dye accumulated (Fig. 1 F). Staining with Direct Red 23 (specific for cellulose) (Fig. 1 I-J) confirmed the presence of cellulose in the mucilage envelope. The highly ordered cellulose was detected in the mucilage of *N.*

pectinata with polarized light microscopy. We observed a strong signal in the envelope that additionally confirmed the presence of cellulose (Fig. 1 K).

Fig. 1

3.2. Seed surface and mucilage arrangement in the dry cell wall of mucilage secreting cells (MSCs)

The seed surface of *L. usitatissimum* is smooth (Fig. 2 A) but the irregular shape of the mucilage secreting cells were visible under higher magnification (Fig. 2 B). *L. usitatissimum* seeds produce a smaller amount of mucilage, in comparison to *N. pectinata* and therefore the deposited mucilage material was visible here only as a thin layer in seed cross sections (Fig. 2 C-D). Rectangular MSCs in *N. pectinata* are organized in tightly arranged ladder-like columns (compare Kreitschitz and Vallès, 2007) which cover the whole seed surface and form the seed coat (Fig. 2 E-F). Abundant mucilage material is deposited at the primary cell walls of MSCs on their surface in the form of densely-packed layers (Fig. 2 G-I).

Fig. 2

3.3. Mucilage architecture after hydration and air drying

After hydration, the mucilage was released from the cells and expanded around the seed in the form of a gel-like envelope. After air drying, the mucilage envelope collapsed and a delicate, transparent layer appeared. Due to its presence, the seeds were 'cemented' to the substrate (cover slip). The mucilage layer of *L. usitatissimum* was rather homogenous in its structure and had only some surface wrinkles resulting from air drying (Fig. 3 A-B). However, in the air-dried mucilage layer of *N. pectinata* (Fig. 3C-D), we observed tightly-packed cellulose strands running either parallel or in different directions (Fig. 3 D). Because the material was very densely organized, it was difficult to estimate the size and shape of individual cellulose fibrils. The wrinkles of dried mucilage were also visible particularly at this place where the mucilage layer expanded from the seed onto the glass surface (Fig. 3 C). Using this method of preparation, only the general morphology of the mucilage envelope was demonstrated.

Fig. 3

3.4. Spatial organization of the seed coat mucilaginous cell wall components after hydration, critical point drying (CPD) and SEM visualization

Using CPD, the spatial organization and interactions of components within the mucilaginous cell wall were shown. We were able to demonstrate the details of the CW at the level of nanostructure and to visualize the size and shape of mucilaginous cell wall

components. Hydration allowed loosening of the cell wall material, which expanded in the form of a 3D network surrounding the seed. The CPD allowed the removal of liquid (alcohol and the remaining water) from the mucilage envelope without strong damage of the network structure of the mucilaginous cell wall components under surface tension.

The mucilage envelope of *L. usitatissimum*, after CPD, had a dense ’crust‘-like structure (Fig. 4 A-B) composed of a few layers (Fig. 4 B). On the seed cross-sections, the material was visible as a compact deposit that adhered to the seed surface (Fig. 4 A). The ’crust’ had many fractures with craggy edges (Fig. 4 B). At higher magnification (Fig. 4 C-E), the mucilage components visible had a form of long, thin fibrils of comparable size, interconnected in a very tangled, irregular network-like structure (Fig. 4 E) spread over the seed surface. In some places, the material was distributed irregular (compacted or loosened), so that the seed surface was visible. The high magnification of *L. usitatissimum* mucilage structure was difficult to obtain because the fibrils were very small and the entire network was very unstable under the electron beam.

Fig. 4

The mucilage envelope of *N. pectinata* after applying CPD was visible as a ‘fluffy’ structure expanded around the seed (Fig. 5 A). The cross-sections of *N. pectinata* seeds showed that the cellulose fibrils were attached to the remaining cell walls of MSCs (Fig. 5 B). Cellulose fibrils were grouped in column-like structures, corresponding to the individual mucilage secreting cells (one column per cell) (Fig. 5 C). All the fibrils looked stretched around the seed, forming a kind of scaffold (Fig. 5 D-E) to which the rest of the components were attached (Fig. 5 E-G).

Fig. 5

Based on width measurements (Tab. 1) we can describe cellulose fibrils as microfibrils and microfibril bundles (Fig. 5 E) with the size varying from 20 nm to 166 nm. The visible microfibrils represented here were the lowest, distinguishable level of the cellulose material (Fig. 6 A-B). Thicker tangled strands (Fig. 5 D) were also noticeable.

Table 1.

Cellulose microfibrils and bundles were covered very compact with fibrillary material i.e. shorter or longer branched chains (Fig. 5 E-G, Fig. 6). Their width ranged from 10,2 nm to 22,58 nm (Tab. 1). The use of the CPD procedure and high resolution SEM at magnifications of up to × 130 000 (Fig. 5 F) and × 200 000 (Fig. 5 G), allowed us to visualize the details. We observed linear and branched shapes of the mucilage components (Fig. 6). Our high resolution images (Fig 5 F-G, Fig. 6) also clearly demonstrated the interaction between

cellulose fibrils and other components. It could be seen that they were cross-linked the cellulose fibrils (Fig. 4) and also covered their surface (Fig. 5 E-G, Fig. 6).

Fig. 6

3.5. Immunolocalization of xylan/arabinoxylan (LM11) and xyloglucan (LM15) epitopes in the mucilage envelope

The control samples of the two studied plant taxa did not show any fluorescence signals in the mucilage envelope. Only a weak signal was observed from the seed surface in both studied taxa (Fig 7 A-D, Fig. 8 A-D). The mucilage envelope of *L. usitatissimum* was visible in the form of small protrusions surrounding the seed (Fig 7 E-G). The immunolabeling with LM11 showed a distinct signal within these protrusions (Fig. 7 E) indicating the presence of xylan/arabinoxylan. The signal was spread homogenously.

The immunolabeling with LM15 for xyloglucan in *L. usitatissimum* showed comparable, strong signal in the same area similar to that previously shown for LM11 i.e. within small mucilage protrusions (mucilage layer) situated on the seed surface (Fig. 7 F-G). Also, the signal was visible in the remaining primary cell walls of the mucilage-secreting cells (Fig. 7 G).

Fig. 7

The results obtained for *N. pectinata* with LM11 and LM15 labeling (Fig. 9) demonstrated clear differences in comparison to *L. usitatissimum*. The control probes did not show any mucilage autofluorescence (Fig. 8 A-D) comparable to that obtained for *L. usitatissimum* seeds.

Fig. 8

The presence of xylan/arabinoxylan, after applying LM11, was detected within the mucilage envelope area (Fig. 9 F-G). The signal was visible in the form of longer or shorter linear segments arranged in long chains (Fig. 9 A-C, Supplement 1).

The results of LM15 labeling for *N. pectinata* indicated the presence of xyloglucan in the primary CW of MSCs (Fig. 9 D-H). After hydration, the swelling of the pectins caused a rupture in the CW of MSCs and the mucilage was then formed. The distinct, homogenous signals were detected in the remainder of the CWs of MSCs, that were spread within the mucilage envelope in the form of small fragments (Fig. 9 D-F) as well as in the remainder of the CWs, that stayed on the seed surface (Fig. 9 G-H).

Fig. 9

4. Discussion

In the study presented here, the detailed spatial organization of the mucilage envelope (mucilaginous cell wall) was revealed. It demonstrated a characteristically loose, net-like arrangement of the components. The pectic mucilage had a fibrillary, tangled and more homogenous structure than the cellulose type. In the case of cellulose mucilage, the main scaffold consisted of long, unbranched cellulose fibrils attached to the seed surface. The rest of the components i.e. shorter, linear and/or branched chains were spread between them and also covered their surface. In addition to structural analysis, immunolocalization of selected hemicelluloses was performed. It showed the presence of these hemicelluloses in specific areas of the mucilage envelope and led to a better understanding of the mucilage structure.

The immunolocalization allowed the detection and localization of the examined hemicelluloses displaying a general pattern of their distribution within the mucilage envelope. The preparation technique used here i.e. CPD and SEM visualization revealed the details of the mucilage spatial microstructure which cannot be shown using traditional staining reactions or immunolocalization. The combination of these two methods also enabled us to attempt transferring the (general) chemical composition of the mucilaginous cell wall onto the direct spatial structural organization. We directly visualized how the cellulose fibrils were attached to the seed surface, how they were organized within the envelope as well as how the components were mutually interactive. Our SEM images directly reproduced the distribution, shape and size of the visualized mucilaginous cell wall components, being well-preserved and distinguishable.

4.1. Microstructure of the mucilage envelope

The presence of cellulose was demonstrated in the mucilage envelope of *Arabidopsis thaliana* using immunolocalization and fluorescence analysis (Macquet et al., 2007; Mendu et al., 2011; Sullivan et al., 2011; Voiniciuc et al., 2015a,b). When interacting with cellulose, the main components of the mucilage envelope are linear or branched polymers represented by pectins (e.g. RG I) and hemicelluloses (xyloglucan, xylan, arabinoxylan) (Zykwinska et al., 2005, 2007; Naran et al., 2008; Scheller and Ulskov, 2010; Pak and Cosgrove, 2012; Western, 2012; Busse-Wicher et al., 2014; Cosgrove, 2014; Voiniciuc et al. 2015a,b). We can surmise that the thin, short (un)branched fibrils, visible in the SEM images, represent the matrix polysaccharides. Presumably, fibrillar material of the flax mucilage, clearly visible in SEM images, may be represented by a mixture of arabinoxylan and RG I detected biochemically in this species previously by Naran et al. (2008). The branched cross-links between cellulose

fibrils in the *Neopallasia pectinata* mucilage envelope may be represented by pectins. The chains covering their surface and cross-linking them may be considered as hemicelluloses.

Our studies revealed the structural differences between two main types of mucilage. Pectic mucilage of *L. usitatissimum* showed disordered spatial organization with tangled and densely-ordered fibrillary components (Fig. 4). The mucilage volume was significantly reduced to form of clusters spread on the seed surface and, in contrast to flax the mucilage of *N. pectinata*, had well-preserved volume and components which were organized in a 3D net-like structure with visible cellulose micro-, macrofibrils and distinctive cross-links (Fig. 5 D-G, 6).

The mucilage material of *L. usitatissimum* (Fig. 4 E) in comparison to *N. pectinata* (Fig. 6 B) was very disordered and densely organized. Fibrils in the flax mucilage were of comparable size, branched, and very tangled. The structural organization of *N. pectinata* mucilage was heterogenous which was visible e.g. in the different size of the fibrilar material (Fig. 6 B). The mucilage skeleton is composed of parallel running, long, unbranched, thick cellulose fibril bundles which split into thinner microfibrils. The cellulose fibrils were covered and crosslinked by thin, short, branched and/or unbranched fibrils, which may represent the matrix polysaccharides. The whole mucilage was loosely organized in the form of a net-like structure.

4.2. Linum usitatissimum – cellulose lacking mucilaginous cell wall

The crust-like structure of the *L. usitatissimum* mucilage was comparable to that of *Arabidopsis thaliana*, which was also revealed using Critical Point Drying and SEM (Windsor et al., 2000). However, the results of this study did not show any such structural details as those seen in our visualizations. A ‘crust’-like mucilage layer was visible around the seed and no cellulose fibrils (identified in A. *thaliana* mucilage) or other fibrillary material were distinguishable (Windsor et al., 2000). Taking the absence of cellulose fibrils in flax mucilage into consideration, we can suppose that our visualizations demonstrated the organization of cell wall matrix polysaccharides (pectins, hemicelluloses) and supported the predicted interaction between them (Heredia et al., 1995; Caffal and Mohnen, 2009). The absence of cellulose, which typically forms a scaffold for the matrix components, could be the reason for such a disordered organization of the mucilage envelope in this instance. In the case of *N. pectinata*, cellulose fibrils formed a very stiff skeleton which was responsible for the anchoring of other mucilage components and maintaining the net-like spatial architecture of the mucilage envelope. In the case of *A. thaliana* (Windsor et al., 2000), we can suppose

that its cellulose fibrils were possibly thin and not strong enough to maintain the mucilage's 3D structure after the CPD procedure.

4.3. Neopallasia pectinata mucilaginous cell wall

The cellulose chains, each of 2 nm width, can associate and form long, unbranched microfibrils (CMF) 8 to 15 nm in width (McCann et al., 1990; Fujino et al., 2000; Caffal and Mohnen, 2009; Zhang et al., 2014). The microfibrils, with an average width of 30 nm, may be visualized by spectroscopic methods (Caffal and Mohnen, 2009). The different size of the cellulose microfibril bundles could possibly be the result of a composite structure containing multiple elementary fibrils and hemicelluloses (Terashima et al., 2009; Donaldson, 2007; Ding et al., 2013). The width of cellulose fibrillary material measured in our study was comparable to the literature data and ranged from 20,66 to 166,06 nm (mean value 60,95 nm). It can therefore be described as cellulose microfibrils and bundles forming elongated aggregations (Fig. 5 E-G, Fig. 6). The presence of crystalline cellulose in *N. pectinata* mucilage (Fig. 1 K) in this instance was supported by analysis in polarized light. The mucilage envelope of *Salvia hispanica* L., studied with AFM, demonstrated tangled, tightly-arranged fibrillary material, described as "mucilage fibres", whose diameter ranged from 15 to 45 nm (Saldago-Cruz et al., 2013) and could also be related to the cellulose fibrils. However, the authors visualized the mucilage envelope at the nanoscale level meaning that their images presented mostly the topography of the sample.

The cellulose microfibrils are coated and cross-linked by hemicelluloses (Fujino et al., 2000; Ding and Himmel, 2006; Terashima et al., 2009; Scheller and Ulskov, 2010). The cellulose bundles of *N. pectinata* in our images were obviously covered by chains of molecules and also cross-linked by them. Fibrillary structures cross-linking the CMF bundles, which were observed in the ginkgo tracheid cell wall, were regarded as hemicelluloses (Terashima et al., 2009). Other authors have also described cross-links between cellulose fibrils which appeared to be hemicelluloses (McCann et al., 1990; Ding et al., 2013). Our results demonstrated the presence of such linear and branched fibrils spread within the scaffold formed by cellulose fibrils. The immunolocalization may support our results with a probability of the presence of hemicelluloses (xylan) in the mucilage envelope interacting with cellulose fibrils.

4.4. Immunolocalization of main hemicellulose characteristic of primary cell wall - Linum usitatissimum

One of the most important hemicelluloses of cell walls are xyloglucans (XG), abundant in primary cell walls (Zykwinska, 2007; Sheller and Ulskov, 2010; Banasiak, 2014; Busse-Wicher et al., 2014; Cosgrove, 2014). Their main function is to tether the cellulose microfibrils together by hydrogen bonding (Marcus et al., 2008; Park and Cosgrove, 2012). Another significant hemicellulose is arabinoxylan, which is an important component of grasses' cell walls and seeds of some dicots such as e.g. flax or psyllium. In the flax mucilage arabinoxylan represents a highly-branched form that is well soluble in water (Naran et al., 2008; Scheller and Ulskov, 2010). Our immunolocalizations showed a very strong signal detecting the presence of xyloglucan in the flax seed mucilage (Fig. 7 F-G). The results of this study differ from the biochemical analysis which detected the presence of diverse monosaccharides and polysaccharides (e.g. arabinoxylan) in the flax seed mucilage but not the presence of xyloglucan (Cui et al., 1994; Fedeniuk and Biliaderis, 1994; Warrand et al., 2005).

In our experiments, we used LM11 as this antibody binds to both unsubstituted xylan and arabinoxylans (McCartney et al., 2005). Given that arabinoxylan is a very characteristic hemicellulose of *Linum usitatissimum* seed mucilage (Fedeniuk and Biliaderis, 1994; Warrand et al., 2005a, b; Naran et al., 2008), we can state that by using the LM11 antibody, we demonstrated its distribution within the flax mucilage envelope. Xyloglucan, characteristic of the PCW, was also detected within the flax mucilage envelope and in the cell wall of the mucilage secreting cells. All of the detected components of flax mucilage could be supposed to be represented by tangled fibrilar material visible in a SEM after CPD. The lack of cellulose can also explain why flax mucilage is adhering poorly to the seed surface (Naran et al., 2008). The results obtained in our experiment suggest that the flax mucilage appears to be a modified primary cell wall with a relatively homogenous structure.

4.5. Immunolocalization of main hemicellulose characteristic of the secondary cell wall - Neopallasia pectinata

Xylans (XY) are less substituted polymers which are characteristic of the secondary cell walls of dicots (Zykwinska, 2007; Sheller and Ulskov, 2010; Banasiak, 2014; Busse-Wicher et al., 2014; Cosgrove, 2014). Their key role is to strengthen the cell wall through additional interactions with cellulose within the mature wall (Caffal and Mohnen, 1990; Sheller and Ulskov, 2010; Busse-Wicher et al., 2014; Voiniciuc et al., 2015b).

Neopallasia pectinata mucilage demonstrated heterogeneity through the presence of cellulose bundles of a different size, covering and cross-linking components. Based on our immunolocalization analyses we could suppose the presence of xylan rather than arabinoxylan

in *N. pectinata* mucilage. Contrary to highly substituted arabinoxylan, xylan is insoluble and should interact with cellulose (Sheller and Ulskov, 2010). We could therefore speculate that our results demonstrated that the fibrillary material covering the cellulose fibrils might correspond to the xylan chains. The cellulose-hemicellulose interaction is well accepted by many authors (Whitheny et al., 1999; Zykwinska et al., 2005, 2007; Caffall and Mohnen, 2009; Altaner and Jarvis, 2008; Scheller and Ulskov, 2010; Busse-Wicher et al., 2014). Altaner and Jarvis (2008), using the 'molecular Velcro' model, simulated interactions of xylan-cellulose associations. In addition a theoretical model of xylan adsorption on cellulose was proposed by Mazeau and Charlier (2012). Our results could provide direct microstructural evidence of the described interaction.

The interaction between pectins and some hemicelluloses such as e.g. xylan or xyloglucan by covalent links were also previously postulated (Caffal and Mohnen, 2009). In seed mucilage of *Arabidopsis thaliana,* xylan chains attached to the RG-I were observed. They can presumably mediate the absorption of mucilage to cellulose fibrils (Ralet et al., 2016; this study).

4.6. Xylan-cellulose interaction in the mucilaginous cell wall - Arabidopsis thaliana vs. Neopallasia pectinata

Xylan contributes to the mechanical strengthening of the cell wall (Scheller and Ulskov, 2010). In recent studies the presence of highly-branched xylan was demonstrated in *Arabidopsis* mucilage. Xylan branches are required to attach the pectins to the seed surface (Hu et al., 2016 a, b; Voiniciuc et al., 2015). Xylan is also necessary for maintaining the cellulose architecture in the mucilage (Voiniciuc et al., 2015b). Our studies revealed the probably specific xylan organization in *Neopallasia pectinata* mucilage as being chains of xylan arranged in longitudinal, individual fibrils (Fig. 9 B-C, Supplement 1). This distribution corresponds to the organization of the cellulose bundles. The cellulose microfibrils as well as the elementary fibrils can be covered by hemicelluloses (Ding and Himmel, 2006). The appearance of the xylan in the mucilage of *N. pectinata* showed a characteristic signal in the form of segments whereas the signal was spread quite homogenously in the mucilage of Arabidopsis. This fact can also demonstrate the diverse character of the xylan structure in both taxa. The interaction between xylan and cellulose fibrils should be responsible for the maintenance of the stiff structure of the mucilage envelope. After CPD, the mucilage of *N. pectinata* did not collapse and "roll up" as in the case of *Linum usitatissimum,* whose mucilage is devoid of cellulose.

4.7. Mucilage envelope – modified cell wall with special properties

The cellulose mucilage, due to the presence of a cellulose skeleton, should be more rigid and should prevent the mucilage from being washed away from the seed surface (Grubert, 1974; Kreitschitz, 2009). It plays an important role in anchoring the mucilage pectin to the seed surface (Harpaz-Saad et al., 2012; Sullivan et al., 2011; Ben-Tov et al., 2015; Voiniciuc et al., 2015a,b). In the case of Arabidopsis the mucilage adherence to the seed surface should also be maintained by other interactions between several wall polymers. Among the already mentioned main mucilage components (cellulose, xylan, RG I) arabinogalactan proteins and galactoglucomannan also play a structural role for the mucilage envelope (Sullivan et al., 2011; Voiniciuc et al., 2015 a, b; Yu et al., 2014).

Our results showed that cellulose fibrils remain attached to the surface after the mucilage is released and serve as a kind of scaffold for the rest of the components. If we consider that the seed coat mucilage represents a modified cell wall, it should not be surprising that the components can be linked together by interactions typical of the cell wall and that the whole mucilage stays attached to the seed surface.

Pectic mucilage, lacking a cellulose skeleton, should be much more exposed to being removed from the seed surface. In experiments where gentle swirling of *Arabidopsis thaliana* mucilaginous seeds was performed, the mucilage outer layer (without cellulose) was dispersed into the medium, whereas the inner layer stayed attached to the seed due to the presence of cellulose (Naran et al., 2008). The studies of *Arabidopsis* mucilage modified mutants suggested that the differences in the branching or cross-linking of other mucilage polysaccharides could also be responsible for the mucilage adhesion (Ralet et al., 2016). Conversely, the pectic mucilage of *Linum usitatissimum* was precipitated into the medium (Naran et al., 2008). Our CPD+SEM visualizations revealed places where the seed was devoid of mucilage and the seed surface was visible. It can also demonstrate the role of cellulose in preventing other components from being lost meaning this fact could also be important e.g. for seed anchoring to the soil or zoochoric seed dispersal (Grubert, 1974; Kreitschitz et al., 2015). The presence of a cellulose (indigestible for many animals), interacting with other cell wall components, prevents the mucilage from being mechanically and/or enzymatically removed during its passage through the digestive system of animals. The specific composition and structure of mucilage can also influence its physical properties e.g. rate of water loss, friction and adhesion (Kreitschitz et al., 2015, 2016) as well as explain its other diverse functions.

4.8. Technical approach and further perspectives in the (mucilage) cell wall structural studies

Standard staining reactions and immunolocalizations serve in the detection and localization of examined components but do not allow us to imagine the spatial and structural details. Revealing the 3D micromolecular architecture of the components in the cell wall requires high-resolution devices such as AFM, SEM, Cryo-SEM. More recently modern technologies as magnetic resonance and electron tomography were also used to study cell wall spatial structure (Nakashima et al., 1997; Marga et al., 2005; Ding and Himmel, 2006; Zimmermann et al., 2006; Sarkar et al., 2009, 2014; Terashima et al., 2009; Lacayo et al., 2010; Dick-Pérez et al., 2011; Wang et al., 2012, 2015). Many techniques often require very extensive sample preparation, which can be destructive to the studied material and provided us only with information about the topography of the studied samples (Sarkar et al., 2009). Considering the difficulties with the structural analysis of the cell wall, we here propose a less-invasive approach which allowed us to demonstrate the seed coat's mucilaginous cell wall micromolecular architecture. The applied methods (CPD+SEM) allowed the well preservation of the studied material and the visualization of its spatial architecture.

The CPD technique is usually used for materials which are either very fragile or wet (Hawkins et al., 2007). Its basic advantage is that it eliminates the problem of surface tension during the drying process (Smith and Finke, 1972; Hawkins et al., 2007). Consequently, after treatment, the material remains without being deformed or its structure collapsing (Hawkins et al., 2007). Using a combination of CPD and SEM, we demonstrated that the mucilaginous cell wall architecture was well-preserved providing us with important and detailed information. The same technique (CPD+SEM) was used for the mucilage morphology of some myxospermatic seeds (Makouate et al., 2012). In this study, only limited information mainly concerning the general morphology of the mucilage envelope, was obtained. On the contrary, we demonstrated that this method can illustrate many details of the studied samples with high precision (high quality images at x400 000 resolution).

The method of spatial structure analysis of the mucilaginous CW demonstrated here can be useful in studying different mutations e.g. of *A. thaliana* defected in cell wall synthesis and composition which are also visible in the seed coat mucilaginous cell wall. It may also be useful for studying the influence of diverse CW-mutations on different CW-functions as well as on its biomechanical attributes, such as adhesion (Kreitschitz et al., 2015, 2016). Finally, the use of seed coat mucilaginous cell wall (due to its specific loose architecture) as a system, which is easy to prepare and visualize using the CPD-SEM technique, can open new possibilities in structural studies of the plant CW.

Conclusions

In the study presented here, we have demonstrated for the first time microstructural organization of seed coat mucilaginous cell wall. The spatial distribution of the mucilaginous cell wall components, their size, shape and the interactions between them were directly visualized using critical point drying (CPD) followed by high resolution scanning electron microscopy (SEM). The studies were complemented by an immunolocalization analysis of selected hemicelluloses, which allowed for a better explanation of the concepts describing the mucilage as a modified primary or secondary cell wall. Our results allowed us to explain how the mucilage structure had an influence on the mucilage envelope function. We can propose the use of seed mucilage for further studies of mucilaginous cell wall spatial architecture due to its easily-accessible nature for microscopy studies and the presence of typical cell wall components. We also believe that the CPD+SEM method utilized can be applied extensively in the future to advance spatial analysis of (mucilaginous) cell wall architecture.

Acknowledgements

We would like to thank Prof. Joan Vallès for the supply of materials, Joachim Oesert for his technical help in CPD and SEM preparations, and to my colleagues from the lab for their critical review of the manuscript. The study was supported by the Short Term Scientific Mission, COST Action TD0906 (COST-STSM-ECOST-STSM-TD0906-020513-030288), by the German Academic Exchange Office (DAAD) (grant No. 323/A/10/02617) and funding from the European Union's Horizon 2020 research and innovation program under the Marie Skłodowska-Curie grant No 702293 – MuCellWall to AK. Victoria Kastner kindly provided linguistic corrections of the manuscript.

Conflict of interest

The authors declare that they have no conflict of interest.

References

Altaner, C.M. and Jarvis, M.C., 2008. Modelling polymer interactions of the 'molecular Velcro' type in wood under mechanical stress. J. Theor. Biol. 253, 434– 445.

Arsovski, A.A., Haughn, G.W., Western, T.L., 2010. Seed coat mucilage cells of *Arabidopsis thaliana* as a model for plant cell wall research. Plant Sign Behav. 5(7), 796–801.

Banasiak, A. 2014. Evolution of the cell wall components during terrestrialization. Acta. Soc. Bot. Pol. 83(4), 349–362.

Ben-Tov, D., Abraham, Y., Stav, S., Thompson, K., Loraine, A., Elbaum, R., de Souza, A., Pauly, M., Kieber, J.J., Harpaz-Saada, S., 2015. COBRA-LIKE 2, a member of the GPI-anchored COBRA-LIKE family, plays a role in cellulose deposition in Arabidopsis seed coat mucilage secretory cells. Plant Physiol. DOI:10.1104/pp.114.240671

Bidlack, J., Malone, M., Benson, R., 1992. Molecular structure and component integration of secondary cell walls in plants. Proc. Okla. Acad. Sci. 72, 51–56.

Busse-Wicher, M., Gomes, T.C.F., Tryfona, T., Nikolovski, N., Stott, K., Grantham, N.J., Bolam, D.N., Skaf, M.S., Dupree, P., 2014. The pattern of xylan acetylation suggests xylan may interact with cellulose microfibrils as a twofold helical screw in the secondary plant cell wall of *Arabidopsis thaliana*. Plant J. 79(3), 492–506.

Caffall, K.H., Mohnen, D., 2009. The structure, function, and biosynthesis of plant cell wall pectic polysaccharides. Carbohyd. Res. 344, 1879–1900.

Capitani, M.I., Ixtaina, V.Y., Nolasco, S.M., Tomás, M.T., 2013. Microstructure, chemical composition and mucilage exudation of chia (*Salvia hispanica* L.) nutlets from Argentina. J. Sci. Food. and Agric. 93(15), 3856–3862.

Cosgrove, D.J., 2014, Re-construction our models of cellulose and primary cell wall assembly. Curr. Opin. in Plant. Biol. 22, 122–131.

Dick-Pérez, M., Zhang, Y., Hayes, J., Salazar, A., Zabotina, O.A., Hong, M. 2011. Structure and interactions of plant cell-wall polysaccharides by two- and three-dimensional magic-angle-spinning solid-state NMR. Biochemistry. 50, 989-1000.

Ding, S-Y., Himmel, M-E., 2006. The maize primary cell wall microfibril: A new model derived from direct visualization. J. Agric. Food. Chem. 54, 597-606.

Ding, S-Y., Zhao, S., Zeng, Y., 2014. Size, shape and arrangement of native cellulose fibrils in maize cell walls. Cellulose. 21, 863-871.

Donaldson, L., 2007. Cellulose microfibril aggregates and their size variation with cell wall type. Wood. Sci. Technol. 41, 443-460.

Fedeniuk, R.W., Biliaderis, C.G., 1994. Composition and physico-chemical properties of linseed (*Linum usitatissimum* L.) mucilage. J. Agric. Food. Chem. 42, 240-247.

Fujino, T., Sone, Y., Mitsuishi, Y., Itoh, T., 2000. Characterization of cCross-links between cellulose microfibrils, and their occurrence during elongation growth in pea epicotyl. Plant Cell. Physiol. 41(4), 486-494.

Grubert, M., 1974, Studies on the distribution of myxospermy among seeds and fruits of Angiospermae and its ecological importance. Acta. Biol..Venez. 8, 315-55.

Harpaz-Saad, S., Western, T.L., Kieber, J.J., 2012. The FEI2-SOS5 pathway and CELLULOSE SYNTHASE 5 are required for cellulose biosynthesis in the Arabidopsis seed coat and affect pectin mucilage structure. Plant. Signal. Behav. 7(2), 285-8.

Heredia, A., Jiménez, A., Guillén, R., 1995. Composition of plant cell walls. Z. Lebensm. Unters. For. 200, 24–31.

Hawkins, D.M., Ellis, E.A., Stevenson, S., Holzenburg, A., Reddy, S.M., 2007. Novel critical point drying (CPD) based preparation and transmission electron microscopy (TEM) imaging of protein specific molecularly imprinted polymers (HydroMIPs). J. Mater. Sci. 42, 9465–9468.

Haughn, G.W., Western, T.L., 2012. *Arabidopsis* seed coat mucilage is a specialized cell wall that can be used as a model for genetic analysis of plant cell wall structure and function. Front. Plant. Sci. 3, 1–5.

Jarvis, M.C. 2009. Plant cell walls: supramolecular assembly, signalling and stress. Struct. Chem. 20, 245–253.

Kreitschitz, A., Vallès, J., 2007. Achene morphology and slime structure in some taxa of *Artemisia* L. and *Neopallasia* L. (Asteraceae). Flora. 202 (7), 570–580.

Kreitschitz, A., 2009. Biological properties of fruit and seed slime envelope – how to live, fly, and not die. In: Gorb. N. S. (ed) Functional surfaces in biology. Berlin et al., Springer, Vol. 1-2, pp.11-30.

Kreitschitz, A., 2012. Mucilage formation in selected taxa of the genus *Artemisia* L. (Asteraceae, Anthemideae). Seed. Sci. Res. 22, 177–189.

Kreitschitz, A., Kovalev, A., Gorb, S.N., 2015. Slipping vs sticking: water-dependent adhesive and frictional properties of *Linum usitatissimum* L. seed mucilaginous envelope and its biological significance. Acta. Biom. 17, 152–159.

Kreitschitz A, Kovalev A, Gorb S.N. 2016. "Sticky invasion" – the physical properties of *Plantago lanceolata* L. seed mucilage. Beilstein J. Nanotechnol. 7, 1918–1927.**Lacayo, C.I., Malkin, A.J., Holman, H-Y.N., Chen, L., Ding, S-Y., Hwang, M.S., Thelen, M.P.,** 2010.

Imaging cell wall architecture in single *Zinnia elegans* tracheary elements. Plant Physiol. 154, 121–133.

Makouate, H.F., Van Rooyen, M.W., Van Der Merwe, C.F., 2012. Anatomy of myxospermic diaspores of selected species in the Succulent Karoo, Namaqualand, South Africa. Bothalia. 42(1), 7–13.

Macquet, A., Ralet. M-C., Kronenberger, J., Marion-Poll, A., North, H.M., 2007. In situ, chemical and macromolecular study of the composition of *Arabidopsis thaliana* seed coat mucilage. Plant Cell. Physiol. 48(7), 984–999.

Marcus, S.E., Verhertbruggen, Y., Hervé, C., Ordaz-Ortiz, J.J., Farkas, V., Pedersen, H.L., Willats, W.G.T., Knox, J.P., 2008. Pectic homogalacturonan masks abundant sets of xyloglucan epitopes in plant cell walls. BMC Plant Biology. 8, 60.

Marga, F., Grandbois, M., Cosgrove, D.J., Baskin, T.I., 2005. Cell wall extension results in the coordinate separation of parallel microfibrils: evidence from scanning electron microscopy and atomic force microscopy. Plant J. 43, 181–190.

Mazeau, K., Charlier, L., 2012. The molecular basis of the adsorption of xylans on cellulose surface. Cellulose. 19, 337–349.

McCann, M.C., Wells, B., Roberts, K., 1990. Direct visualization of cross-links in the primary plant cell wall. J. Cell. Sci. 96, 323–334.

McCann, M.C., Roberts, K., 1991. Architecture of the primary cell wall. In: Lloyd CW (ed.) The cytoskeletal basis of plant growth and form. Toronto, Canada, Academic Press.

McCartney, L., Marcus, S.E., Knox, J.P., 2005. Monoclonal antibodies to plant cell wall xylans and arabinoxylans. J. Histochem. Cytochem. 53, 543–546.

Mendu, V., Griffiths, J., Persson, S., Stork, J., Downie, B., Voiniciuc, C., Haughn, G., DeBolt, S., 2011. Subfunctionalization of cellulose synthases in seed coat epidermal cells mediate secondary radial wall synthesis and mucilage attachment. Plant Physiol. 157, 441–453.

Mohnen, D., 2008. Pectin structure and biosynthesis. Curr Opin Plant Biol. 11, 266–77.

Mühlethaler, K., 1950. The structure of plant slimes. Exp. Cell. Res. 1, 341–350.

Nakashima, J., Mizuno, T., Takabe, K., Fujita, M., Saiki, H., 1997. Direct visualization of lignifying secondary wall thickenings in *Zinnia elegans* cells in culture. Plant Cell Physiol. 38(7), 818–827.

Naran, R., Chen, G., Carpita, N.C., 2008. Novel rhamnogalacturonan I and arabinoxylan polysaccharides of Flax seed mucilage. Plant Physiol. 148, 132–141.

North, H.M., Berger, A., Saez-Aguayo, S., Ralet, M-C., 2014. Understanding polysaccharide production and properties using seed coat mutants: future perspectives for the exploitation of natural variants. Ann. Bot. 114, 1251-63.

Park, Y.B., Cosgrove, D.J., 2012. Changes in cell wall biomechanical properties in the xyloglucan-deficient xxt1/xxt2 mutant of *Arabidopsis*. Plant Physiol. 158(1), 465–475.

Pelloux, J., Rustérucci, C., Mellerowicz, E.J., 2007. New insights into pectin methylesterase structure and function. Trends. Plant. Sci. 12(6), 267–277.

Ralet, M-C., Crépeau, M-J., Vigouroux, J., Tran, J., Berger, A., Sallé, C., Granier, F., Botran, L., North, H.M. 2016. Xylans provide the structural driving force for mucilage adhesion to the Arabidopsis seed coat. Plant Physiol. 171, 165–178.

Salgado-Cruz, Ma. de la Paz, Calderón-Domínguez, G., Chanona-Pérez, J., Farrera-Rebollo, R.R., Méndez-Méndez, J.V., Díaz-Ramírez, M., 2013. Chia (*Salvia hispanica* L.) seed mucilage release characterisation. A microstructural and image analysis study. Ind. Crop. Prod. 51, 453-462.

Sarkar. P., Bosneaga, E., Auer, M., 2009. Plant cell walls throughout evolution: towards a molecular understanding of their design principles. J. Exp. Bot. 60(13), 3615–3635.

Sarkar, P., Bosneaga, E., Yap, E.G. Jr, Das, J., Tsai, W-T., Cabal, A., Neuhaus, E., Maji, D., Kumar, S., Joo, M., Yakovlev, S., Csencsits, R., Yu, Z., Bajaj, C., Downing, K.H., Auer, M., 2014. Electron tomography of cryo-immobilized plant tissue: a novel approach to studying 3D macromolecular architecture of mature plant cell walls in situ. PLoS ONE. 9(9), 1–16.

Satiat-Jeunemaitre, B., Martin, B., Hawes, C., 1992. Plant cell wall architecture is revealed by rapid-freezing and deep-etching. Protoplasma. 167, 33–42

Scheller, H.V., Ulvskov, P., 2010. Hemicelluloses. Annu. Rev. Plant. Biol. 61, 263–89.

Smith, M.E., Finke, E.H., 1972. Critical point drying of soft biological material for the scanning electron microscope. Invest. Ophth. 11(3), 127–132.

Somerville, C., Bauer, S., Brininstool, G., Facette, M., Hamann, T., Milne, J., Osborne, E., Paredez, A., Persson, S., Raab, T., Vorwerk, S., Youngs, H., 2004. Toward a systems approach to understanding plant cell walls. Science. 306, 2206–2211.

Sullivan, S., Ralet, M.C., Berger, A., Diatloff, E., Bischoff, V., Gonneau, M., Marion-Poll, A., North, H.M., 2011. CESA5 is required for the synthesis of cellulose with a role in structuring the adherent mucilage of *Arabidopsis* seeds. Plant Physiol. 156, 1725–1739.

Terashima, N., Kitano, K., Kojima, M., Yoshida, M., Yamamoto, H., Westermark, U., 2009. Nanostructural assembly of cellulose, hemicellulose, and lignin in the middle layer of secondary wall of ginkgo tracheid. J. Wood. Sci. 55, 409–416.

Voiniciuc, C., Dean, G.H., Griffiths, J.S., Kirchsteiger, K., Hwang, Y.T., Gillett, A., Dow, G., Western, T.L., Estelle, M., Haughn, G.W., 2013. FLYING SAUCER1 is a transmembrane RING E3 ubiquitin ligase that regulates the degree of pectin methylesterification in Arabidopsis seed mucilage. Plant Cell. 25, 944-59.

Voiniciuc, C., Yang, B., Schmidt, MH-W., Günl, M., Usadel, B., 2015a. Starting to gel: how *Arabidopsis* seed coat epidermal cells produce specialized secondary cell walls. Int. J. Mol. Sci. 16, 3452–3473.

Voiniciuc, C., Günl, M., Schmidt, MH-W., Usadel, B., 2015b. Highly branched xylan made by IRX14 and MUCI21 links mucilage to Arabidopsis seeds. Plant Physiol. doi:10.1104/pp.15.01441

Wang, T., Zabotina, O., Hong, M., 2012. Pectin-cellulose interactions in the Arabidopsis primary cell wall from two-dimensional magic-angle-spinning solid-state nuclear magnetic resonance. Biochemistry. 51, 9846-9856.

Wang, T., Park, Y.B., Cosgrove, D.J., Hong, M., 2015. Cellulose-pectin spatial contacts inherent to never-dried Arabidopsis primary cell walls: evidence from solid-state nuclear magnetic resonance. Plant Physiol. 168(3), 871-84.

Warrand, J., Michaud, P., Picton, L., Muller, G., Courtois, B., Ralainirina, R., Courtois, J., 2005a. Structural investigations of the neutral polysaccharide of *Linum usitatissimum* L. seeds mucilage. Int. J. Biol. Macrom. 35, 121–125.

Warrand. J., Michaud, P., Picton, L., Muller, G., Courtois, B., Ralainirina, R., Courtois, J., 2005b. Contributions of intermolecular interactions between constitutive arabinoxylans to the flaxseeds mucilage properties. Biomacromolecules. 6, 1871–1876.

Western, T.L., 2012. The sticky tale of seed coat mucilages: production, genetics, and role in seed germination and dispersal. Seed. Sci. Res. 22, 1-25.

Whitney, S.E.C., Gothard, M.G.E., Mitchell, J.T., Gidley, M.J., 1999. Roles of cellulose and xyloglucan in determining the mechanical properties of primary plant cell walls. Plant Physiol. 121, 657–663.

Willats, W.G.T., McCartney, L., Knox, J.P., 2001. In-situ analysis of pectic polysaccharides in seed mucilage and at the root surface of *Arabidopsis thaliana*. Planta. 213, 37–44.

Windsor, J.B., Symonds, V.V., Mendenhall, J., Lloyd, A.L., 2000. *Arabidopsis* seed coat development: morphological differentiation of the outer integument. Plant J. 22, 483–493.

Hu R., Li, J., Wang, X., Zhao, X., Yang, X., Tang, Q., He, G., Zhou, G., Kong, Y. 2016 a. Xylan synthesized by Irregular Xylem 14 (IRX14) maintains the structure of seed coat mucilage in Arabidopsis. J. Exp. Bot. 67(5), 1234-1257.

Hu, R., Li, J., Yang, X., Zhao, X., Wang, X., Tang, Q., He, G., Zhou, G., Kong, Y. 2016 b. Irregular xylem 7 (IRX7) is required for anchoring seed coat mucilage in Arabidopsis. Plant Mol. Biol. 92, 25–38.

Young, R.E., Mcfarlane, H.E., Hahn, M.G., Western, T.L., Haughn, G.W., Samuels, A.L., 2008. Analysis of the Golgi apparatus in *Arabidopsis* seed coat cells during polarized secretion of pectin-rich mucilage. Plant Cell. 20, 1623–1638.

Yu. L., Shi, D., Li, J., Kong, Y., Yu, Y., Chai, G., Hu, R., Wang, J., Hahn, M.G., Zhou, G., 2014. CSLA2, a glucomannan synthase, is involved in maintaining adherent mucilage structure in Arabidopsis seed. Plant Physiol. 164, 1842-1856.

Zhang, T., Mahgsoudy-Louyeh, S., Tittmann, B., Cosgrove, D.J., 2014. Visualization of the nanoscale pattern of recently-deposited cellulose microfibrils and matrix materials in never-dried primary walls of the onion epidermis. Cellulose. 21(2), 853-862.

Zimmermann, T., Thommen, V., Reimann, P., Hug, H.J., 2006. Ultrastructural appearance of embedded and polished wood cell walls as revealed by atomic force microscopy. J. Struct. Biol. 156, 363–369.

Zykwinska, A.W., Ralet, M-C.J., Garnier, C.D., Thibault, J-F.J., 2005. Evidence for in vitro binding of pectin side chains to cellulose. Plant. Physiol. 139, 397–407.

Zykwinska, A.W., Thibault, J-F.J., Ralet, M-C.J., 2007. Organization of pectic arabinan and galactan side chains in association with cellulose microfibrils in primary cell walls and related models envisaged. J. Exp. Bot. 58(7), 1795–1802.

Figures

Fig. 1. Morphology of the mucilage envelope

A-C. *Linum usitatissimum***; A.** Narrow mucilage envelope visible after hydration; **B-C.** Mucilage envelope stained with ruthenium red for pectins; **D-K** *Neopallasia pectinata*; **D.** Unstained mucilage envelope. Delicate color comes from cellulose fibrils which are imbeded in the mucilage mass; **E.** Staining with ruthenium read revealed the presence of pectins; also delicate cellulose fibrils are also visible; **F-H**. Staining with safranin for pectins and cellulose; **F.** Mucilage formed abundant envelope around the seed; **G-H.** Coiled cellulose fibrils; **I-J.** Specific staining with Direct Red 23 for cellulose. Visible red color of cellulose microfibrils; **K.** Unstained mucilage visible in polarized light. Strong signal indicates the presence of crystalline cellulose. Abbreviations: cc – crystalline cellulose, me – mucilage envelope. Scale bar: A, B, F 1 mm, C, E 200 μm, D, I, K 500 μm, G, J 100 μm, H 50 μm.

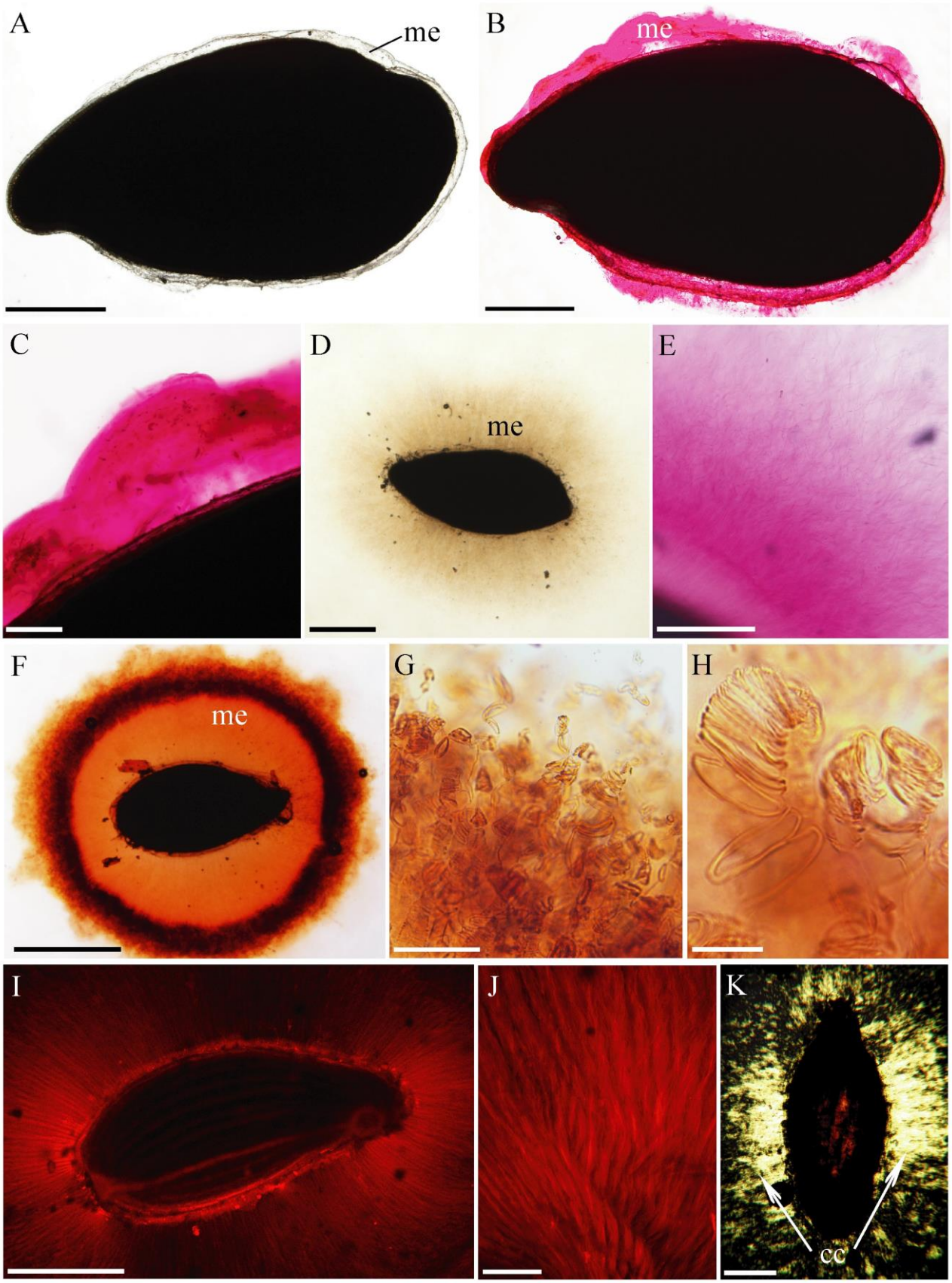

Fig. 2. Morphology of dry seeds and mucilage layer arrangement in mucilage secreting cells

A-D. *Linum usitatissimum***; E-I.** *Neopallasia pectinata***; A.** *L. usitatissimum* seed; **B.** Seed surface with marked outlines of the mucilage secreting cells; **C-D.** Cross fracture of the dry seed with a visible, thin layer of the mucilage material; **E.** *Neopallasia pectinata* seed covered over its entire surface with the mucilage secreting cells; **F.** Fragment of the ladder-like column with marked outlines of rectangular mucilage secreting cells; **G-I.** Cross fracture of the dry seed; visible thick layers of deposited mucilage of the mucilage secreting cells. Abbreviations: **dmu** – deposited mucilage, **MSCs** – mucilage secreting cells.

Scale bars: A - 1 mm; B, D - 100 μm; C - 200 μm, E - 500 μm; G, F - 50 μm; H - 40 μm; I - 20 μm.

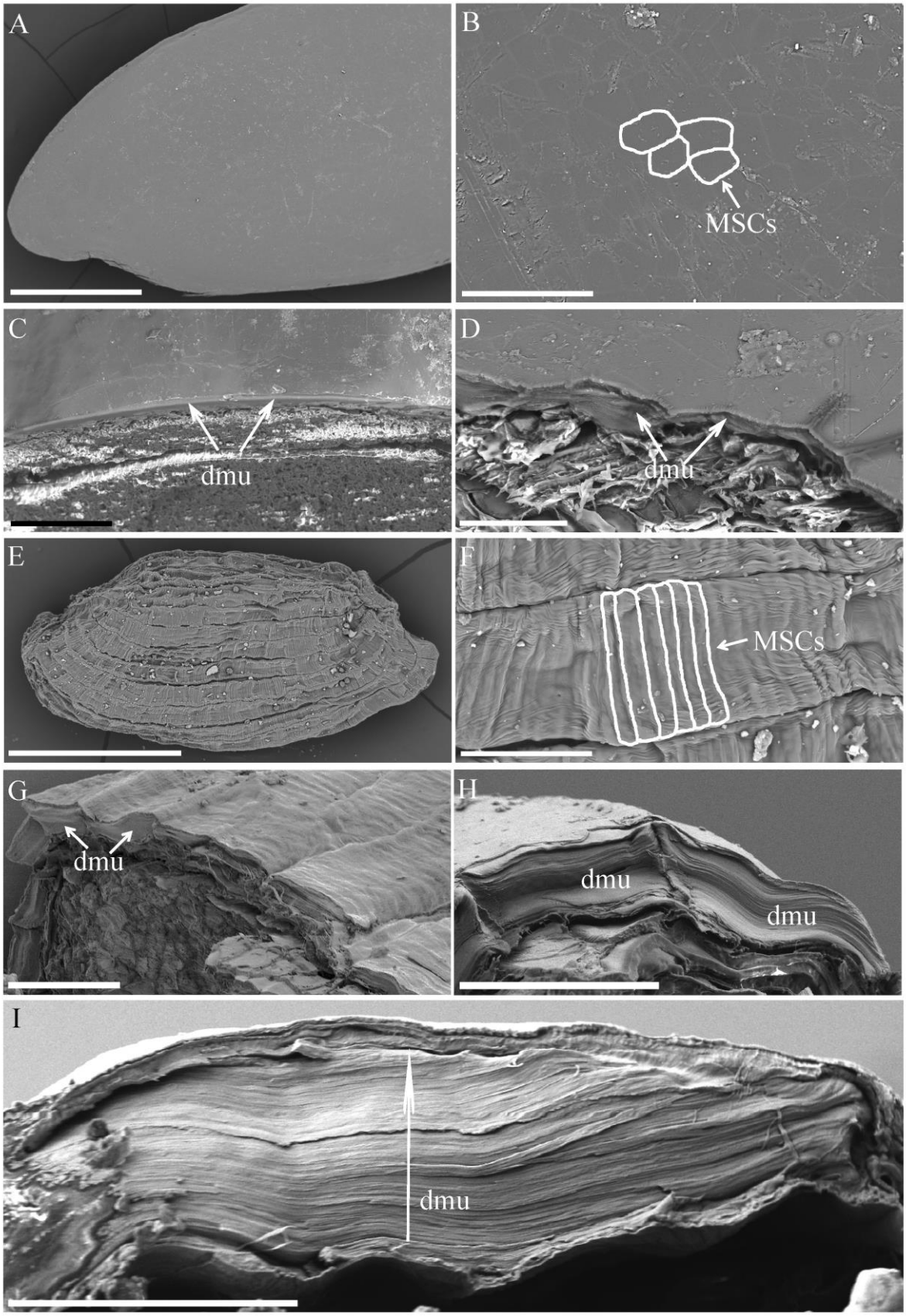

Fig. 3. Morphology of hydrated and air dried mucilage envelope in SEM images

A-B. Hydrated and air dried mucilage envelope of *Linum usitatissimum;* **A**. Visible mucilage envelope (arrow) surrounding the seed and "cementing" it to the glass surface; **B**. Homogenous, smooth structure of mucilage envelopevisible some wrinkles and fractures of the mucilaginous material; **C-D.** Air-dried mucilage of *N. pectinata*; **C**. Seed with mucilage envelope cemented to the glass surface, wrinkles of the dried, expanded mucilage are visible (arrows); **D.** High magnification image of mucilage envelope; cellulose fibrils are very densely arranged within the mucilage and run either parallel or in different directions. Abbreviations: **cf** – cellulose fibrils, **me** – mucilage envelope, **mw** – mucilage wrinkles, **se** – seed,. Scale bars: A- 1 mm; B - 100 μm; C - 500 μm; D - 5 μm. ;

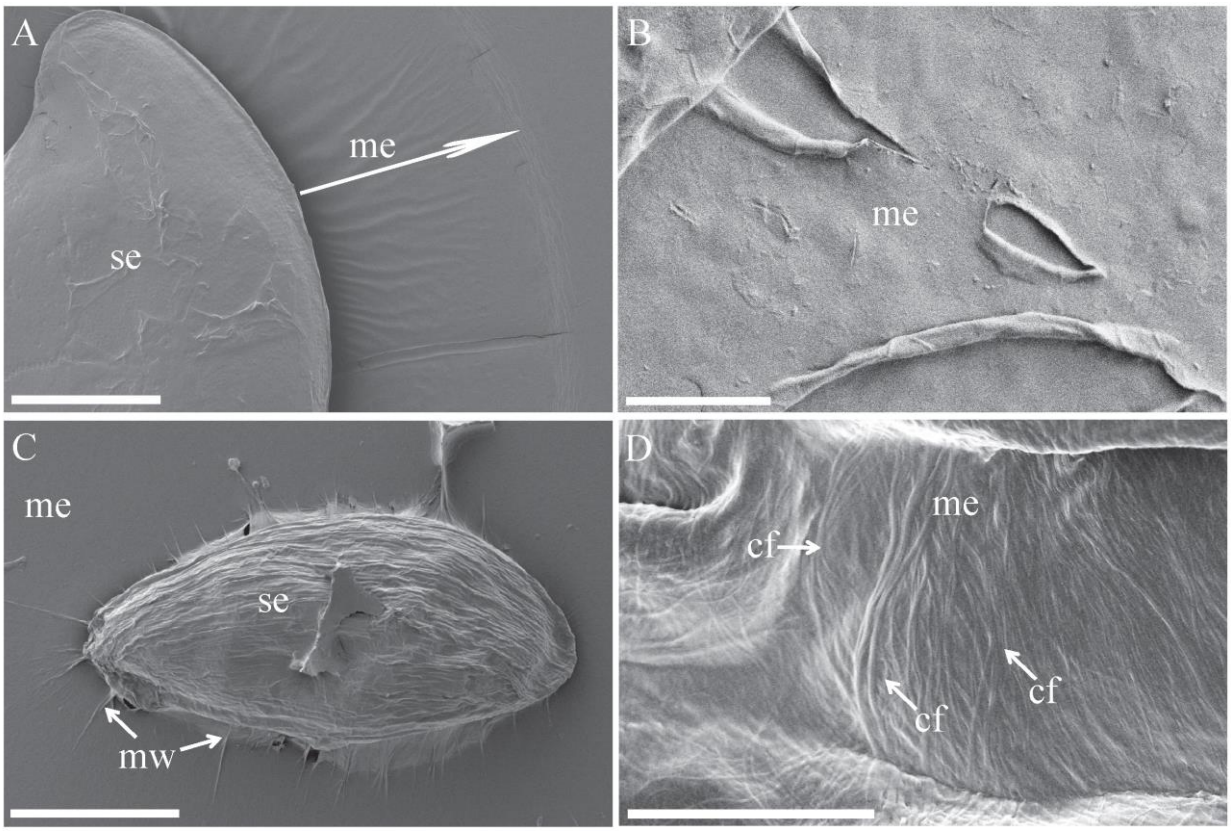

Fig. 4. Critical Point Dried (CPD) preparations of hydrated *Linum usitatissimum* mucilage envelope, SEM images

A. Seed cross-section showing the mucilage envelope tightly adhering to the seed surface in a form of compact layer; **B**. Magnification image demonstrating the crust-like character of the mucilage, visible fibril fractures, and layer arrangement within the envelope; **C-D.** Close up of mucilage demonstrating its irregular, net-like structure, and homogeneity of the fibril size; clumps of mucilage material are also visible; **E**. Fibrillary mucilaginous material arranged in a tangled, net-like structure. Abbreviations: **me** – mucilage envelope. Scale bars: A - 1 mm; B - 200 μm; C - 40 μm; D - 30 μm; E - 500 nm.

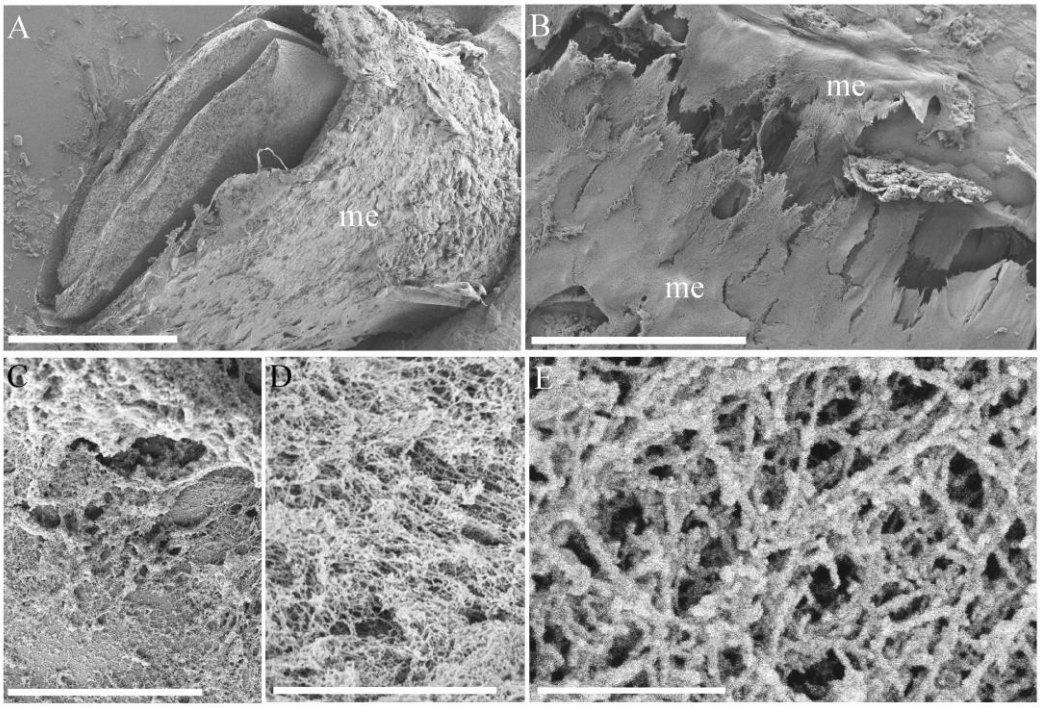

Fig. 5. Critical Point Dried (CPD) preparations of *Neopallasia pectinata* mucilage envelope, SEM images

A. Seed cross-section showing 'fluffy' structure of mucilage formed by cellulose fibrils; mucilage envelope is very abundant; **B**. Cellulose fibrils are attached (arrow heads) to the remaining cell wall (arrows) of mucilage secreting cells. **C**. High magnification image showing the envelope dried in a stretched condition where fibril bundles are arranged in column-shaped structures; **D-E.** Chains of mucilage material visible as thick strands running in different directions, but sometimes also parallel. **E**. Visible cellulose fibrils aggregating into thicker bundles and spread between them cross-linking other mucilaginous components (arrows); **F-G.** High resolution images show fragment of the cellulose fibril; **F**. Cellulose macrofibril splitting in microfibrils; the macrofibril is covered with fibrillary material (arrows); chains of other fibrillary material (probably matrix polysaccharides, arrows) are also visible. **G**. Fragment of microfibril (arrow); a probably linking matrix polysaccharide chain expanded between cellulose microfibrils is visible (arrow). Abbreviations: **cfb** – cellulose fibril bundles, **cl** – column, **cm** – cellulose microfibril, **csp** – cross-linking polysaccharides, **cp** – covering polysaccharides, **cw** – cell wall, **me** – mucilage envelope, **se** - seed. Scale bars: A - 1 mm; B - 40 μm; C - 20 μm; D - 100 μm; E - 5 μm; F - 1 μm; G - 400 nm.

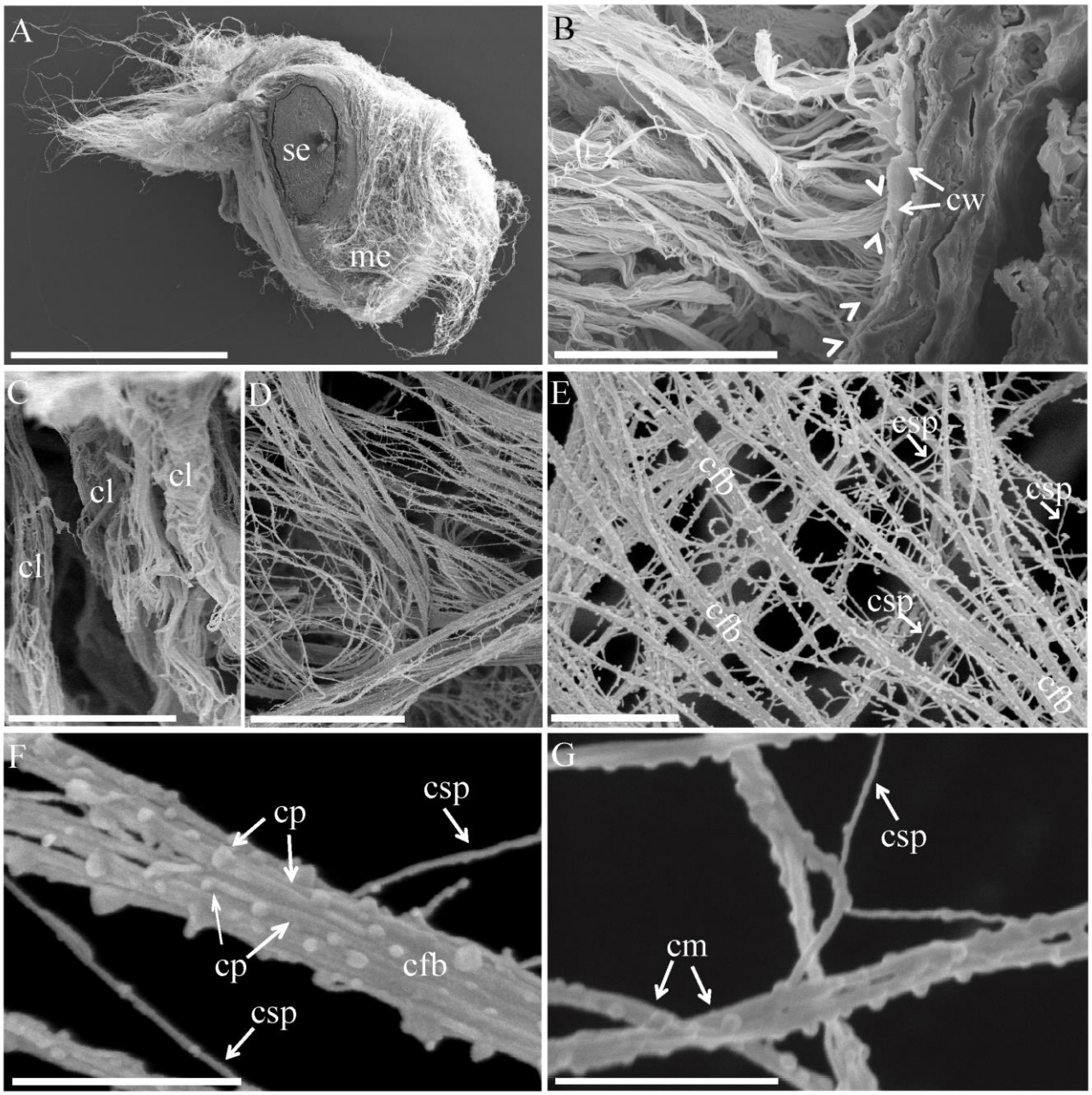

Fig. 6. High magnification SEM images of *Neopallasia pectinata* mucilage after CPD showing spatial distribution of mucilaginous cell wall components

A. Mucilage fragment with visible spatial, net-like organization of polysaccharides; cellulose fibril bundles and microfibrils (arrows) presumably with matrix polysaccharides expanded between them; the rectangle shows the magnified area presented in B; **B.** Cellulose microfibril bundles and microfibrils are covered with fibrilar material (probably matrix polysaccharides, arrows); cross-linking (probably) matrix polysaccharides (arrowheads) are visible between cellulose fibrils. Abbreviations: **cfb** – cellulose fibril bundles, **cm** - cellulose microfibril, **csp** – cross-linking polysaccharides, **cp** – covering polysaccharides. Scale bars: A - 1 μm; B - 500 nm.

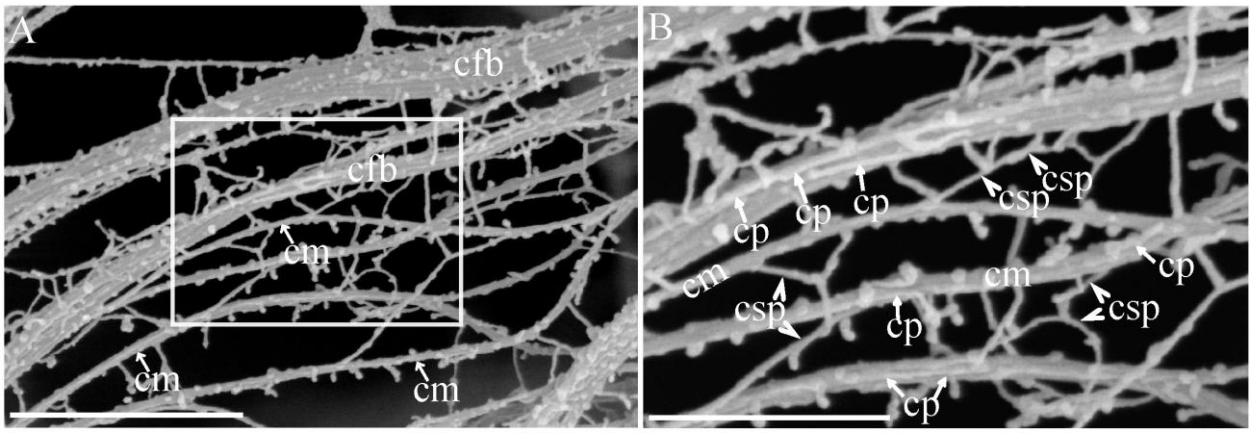

Fig. 7. Immunolocalization of arabinoxylan and xyloglucan in the *Linum usitatissimum* mucilage envelope

A-D. Control probes showing no fluorescence of the mucilage; **E**. Immunolocalization of arabinoxylan with LM11. Signal is located in the mucilage envelope (arrows) attached to the seed; **F-G.** Immunolocalization of xyloglucan with LM15; **F.** The signal is spread in the mucilage covering the seed surface (arrows); **G**. A signal is visible in the remains of the cell walls of mucilage-secreting cells (arrows). Abbreviations: **XG** – xyloglucan. Scale bars: A, E - 500 μm; B-D, F-G - 200 μm,

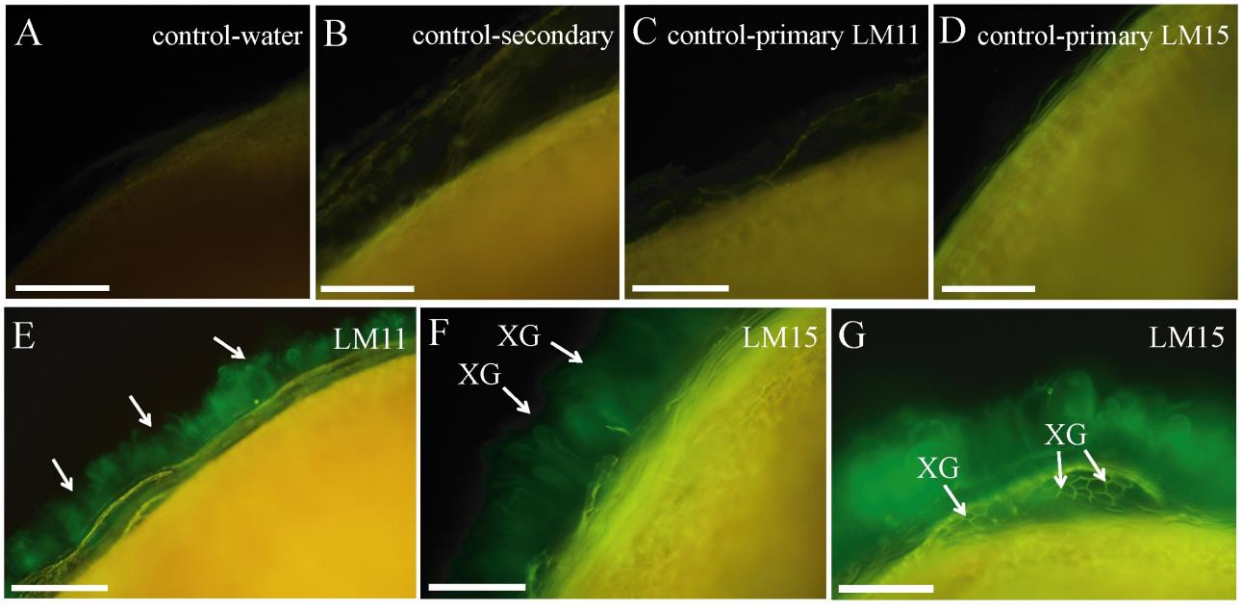

Fig. 8. Immunolocalization of xylan and xyloglucan in the *Neopallasia pectinata* mucilage envelope – control probes

A-B. Control probes with water and a secondary antibody showing no autofluorescence of the mucilage; **C.** Control probe for LM11 showing no autofluorescence of the mucilage; **D.** Control probe for LM15 showing no autofluorescence of the mucilage; Scale bars: A-D - 500 µm.

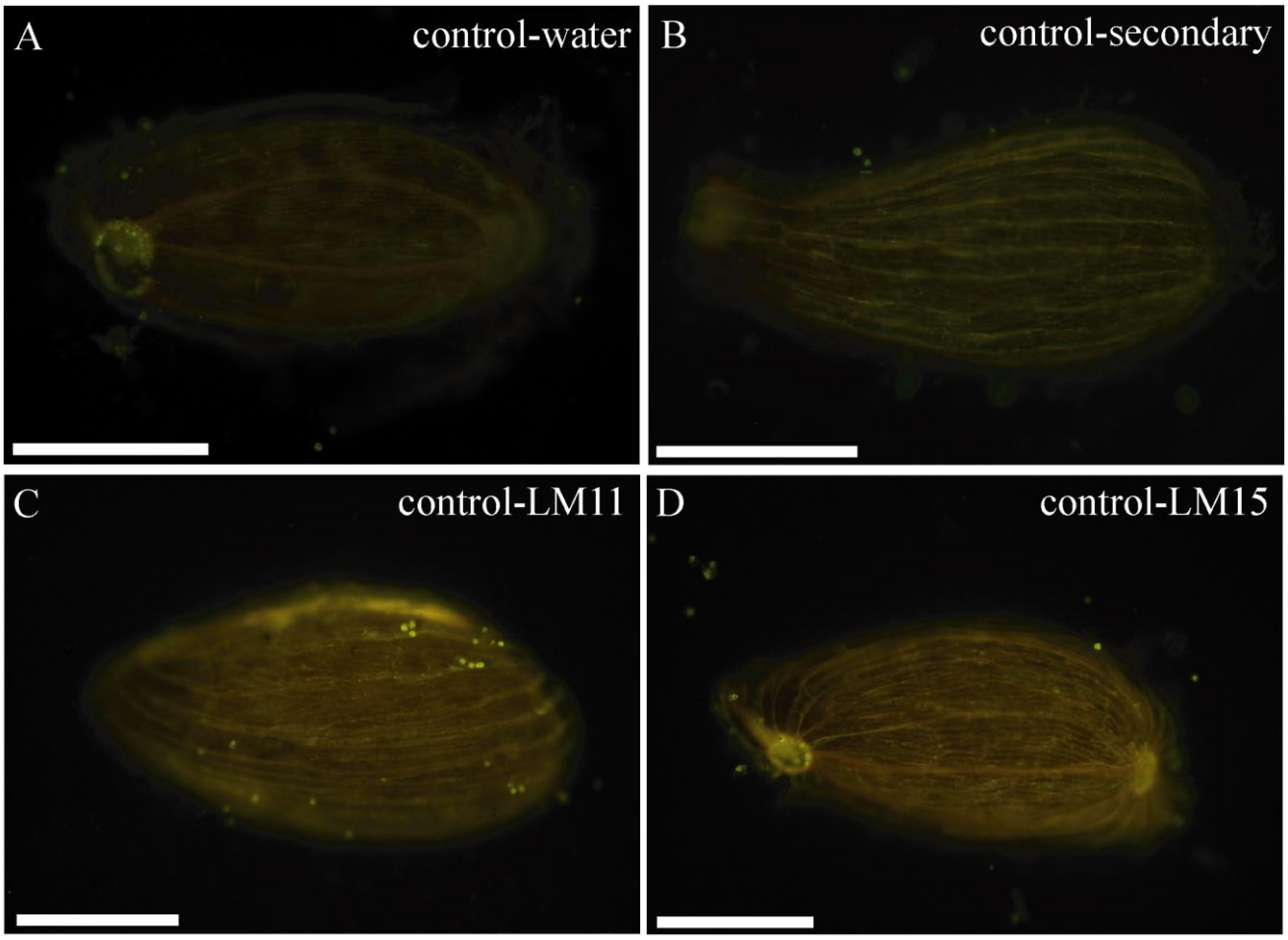

Fig. 9. Immunolocalization of xylan and xyloglucan in the *Neopallasia pectinata* mucilage envelope

A-C. Immunolocalization with LM11; **A.** The mucilage envelope is spread over the seed; a strong signal, coming from the xylan located within the mucilage, is visible; **B.** Stretched, coiled cellulose fibrils in the mucilage envelope covered with xylan; the signal is visible as longer or shorter linear segments arranged in long chains (arrows); **C**. Coiled cellulose fibrils covered with chains of xylan (arrows); **D-H.** Immunolocalization with LM15; **D-F.** Seed surrounded by the mucilage envelope; many small green signals (arrows) showed the presence of xyloglucan in the fragments of the primary cell wall of mucilage secreting cells (MSCs); small fragments of broken cell walls are spread over the mucilage envelope; **G-H.** Signal indicates the presence of xyloglucan in the fragments of the cell walls (arrows) of MSCs which are also visible on the seed surface, where they stay attached. Abbreviations: **cf** – cellulose fibrils; **me** – mucilage envelope, **se** – seed, **XG** – xyloglucan, **XY** – xylan. Scale bars: A, E-G - 200 μm; B-C, H - 50 μm; D - 500 μm.

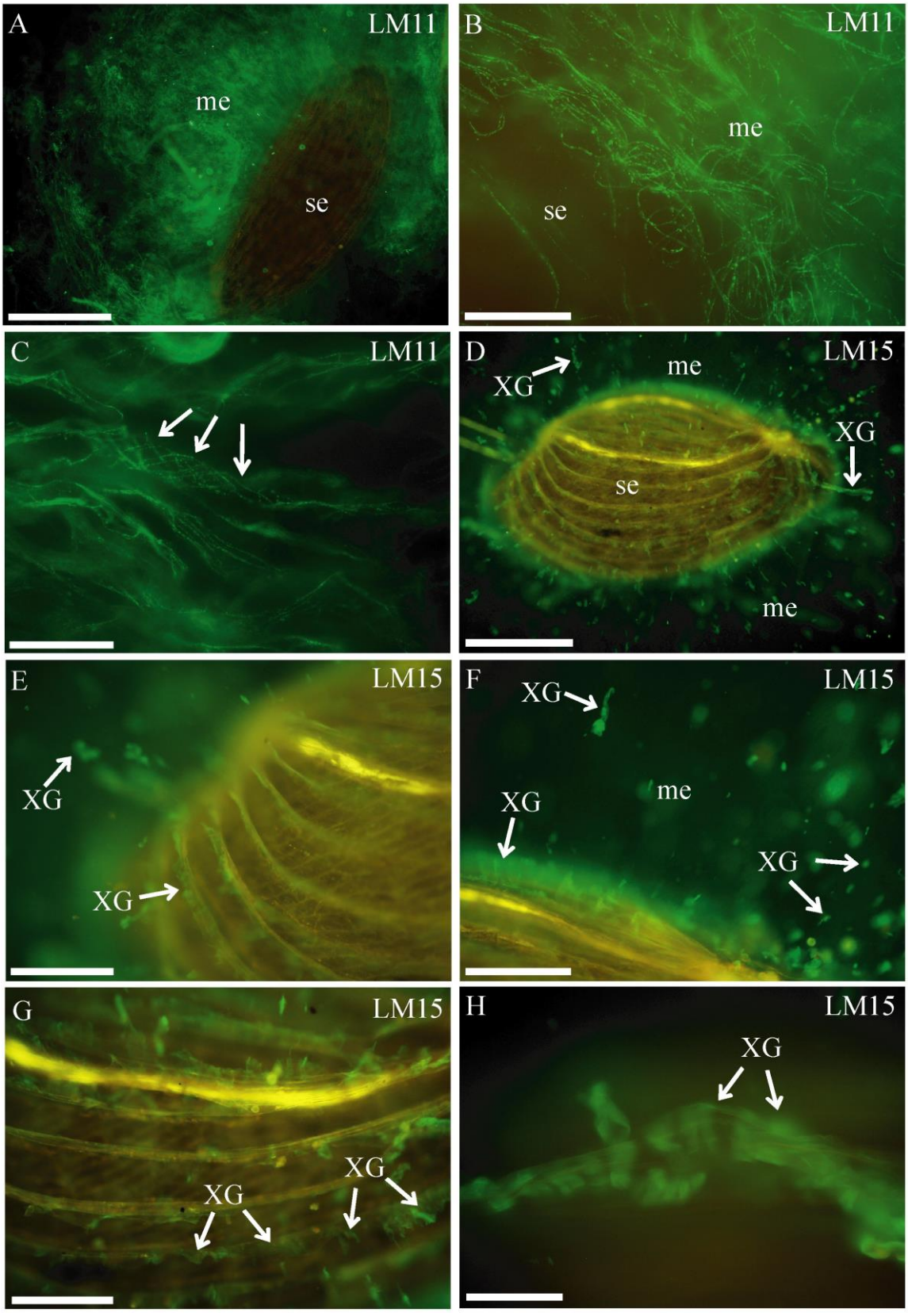

Table 1. Width measurements of fibrillary material of *Neopallasia pectinata*

Measured structure	Minimal width [nm]	Maximal width [nm]	Mean value [nm]	Standard deviation	Count of measurements
Cellulose bundles	20,66	166,06	60,24	±37,64	52
Cross-links	10,2	22,58	16	±2,54	88